Published in final edited form as:
*Biochemistry*. 2011 December 27; 50(51): 11015–11024. doi:10.1021/bi2016102.

# Lipid-mediated unfolding of 3-beta hydroxysteroid dehydrogenase2 is essential for steroidogenic activity

**Maheshinie Rajapaksha**[1], **James L. Thomas**[2], **Michael Streeter**[3], **Manoj Prasad**[1], **Randy M. Whittal**[4], **John D. Bell**[3], and **Himangshu S. Bose**[1]

[1] Mercer University School of Medicine and Memorial University Medical Center, Savannah, GA 31404

[2]Division of Basic Medical Sciences, Mercer University School of Medicine, Macon, GA 31207

[3]Department of Physiology and Developmental Biology, Brigham Young University, Provo, Utah 84602

[4]Department of Chemistry, University of Alberta, Edmonton, Alberta, Canada T6G 2G2

## Abstract

For inner mitochondrial membrane (IMM) proteins that do not undergo N-terminal cleavage, their activity may occur in the absence of a receptor present in the mitochondrial membrane. One such protein is human 3-beta hydroxysteroid dehydrogenase-2 (3βHSD2), the IMM resident protein responsible for catalyzing two key steps in steroid metabolism: the conversion of pregnenolone to progesterone and dehydroepiandrosterone (DHEA) to androstenedione. Conversion requires that 3βHSD2 serves as both a dehydrogenase and isomerase. The dual functionality of 3βHSD2 results from a conformational change, but the trigger for this change remains unknown. Using Fluorescence Resonance Energy Transfer (FRET), we found that 3βHSD2 interacted strongly with a mixture of dipalmitoylphosphatidylglycerol (DPPG) and dipalmitoylphosphatidylcholine (DPPC). 3βHSD2 became less stable when incubated with the individual lipids, as indicated by the decrease in thermal denaturation (Tm), from 42° C to 37° C. DPPG, alone or in combination with DPPC, led to a decrease in α-helical content without affecting the β-sheet conformation. With the exception of the N-terminal 20 amino acids, mixed vesicles protected 3βHSD2 from trypsin digestion. However, protein incubated with DPPC was only partially protected. The lipid-mediated unfolding completely supports the model in which a cavity forms between the α-helix and β-sheet. As 3βHSD2 lacks a receptor, opening the conformation may activate the protein.

A large number of mitochondrial proteins contain targeting information within regions of the mature protein rather than in a cleavable presequence. Proteins that lack a cleavable presequence include all of the outer mitochondrial membrane (OMM) proteins, the majority of inner mitochondrial membrane (IMM) proteins, numerous multi-spanning inner membrane proteins, as well as a few matrix proteins. Some inner membrane proteins contain an internal, positively charged “presequence”-like signal that is often preceded by a hydrophobic sequence. Translocation of these proteins through the mitochondria may require that the positively charged sequence form a loop structure (*1*). Reconstitution experiments have revealed the minimum requirement for integration of preproteins into the

Address all correspondence to: Himangshu S. Bose, Department of Biochemistry, Division of Biomedical Science, Mercer University School of Medicine and Memorial University Medical Center, Hoskins Research Building, 4700 Waters Avenue, Savannah, GA 31404, Tel: 912 350 1710; Fax: 912 350 1765; bose_hs@mercer.edu and bosehi1@memorialhealth.com.

Supplemental Information: Mass spectrometric analysis (Tables) is presented separately as supporting information. Supplemental materials may be accessed free of charge online at http://pubs.acs.org.

IMM: the translocase complex, Tim23; a highly negatively charged lipid membrane, which was not surprising given that negatively charged cardiolipin represents the characteristic dimeric phospholipid of mitochondrial membranes; and lastly, a membrane potential (*2*). Preproteins that insert into the IMM via Tim23 contain a matrix-targeting signal followed by a hydrophobic sorting signal. This sorting signal arrests translocation in the IMM, causing a lateral release of the protein into the lipid phase of the membrane (*3*). The conformation of these proteins is determined by the energetic information specified within their sequences and the process generally involves a variety of intermediate states with decreasing free energies. These mitochondrial membrane proteins often have a β-barrel structure, similar to gram negative bacterial proteins. *In vitro* studies using bacterial β-barrel proteins have shown that insertion results in "molten-disc" intermediates that have a partial secondary structure with the β-strands sitting flat on the membrane surface (*4*). The formation of these intermediates also likely occur in mitochondrial membrane proteins as bacterial proteins expressed in yeast translocate into the mitochondria using the same pathway as eukaryotic proteins, thus demonstrating conservation of the membrane insertion pathway (*5*).

Lipids play a vital role in the conformation of IMM proteins, and they are necessary for both the function of translocase complexes (*2*) and the insertion of precursor proteins (*6, 7*). The dimeric phospholipid cardiolipin, a major component of the IMM, is of critical importance for the organization and function of many protein complexes in the membrane, including presequence translocases (*2, 8, 9*). The lipid composition of the different mitochondrial compartments changes because phospholipid transport, similar to protein transport, can occur at contact sites between the OMM and IMM (*10, 11*), and thus lipids may influence the activity of a protein (*12*).

Cells do not store steroids, but instead synthesize them based on physiological demand. 3-beta hydroxysteroid dehdrogenase (3βHSD2) (*13*) is a steroidogenic enzyme present at the IMM (*14*). This enzyme, which lacks a heme group and requires $NAD^+$ as a cofactor, catalyzes the production of many steroids: pregnenolone to progesterone, 17α-hydroxy pregnenolone to 17α-hydroxy progesterone, and dehydroepiandrosterone (DHEA) to androstenedione. Enzymes involved in this pathway are present in all steroidogenic tissues as well as some non-steroidogenic tissues, such as kidney and skin. In humans, 3βHSD2 is specifically expressed in the adrenal gland, ovary and testis (*13*), and is required for the production of cortisol, aldosterone and sex hormones (*15*). 3βHSD converts pregnenolone to progesterone and DHEA to androstenedione (Fig 1A) through dehydrogenase and isomerase reactions. Because of the central role in steroidogenesis, changes in 3βHSD activity can have a wide range of effects: progesterone imbalance can affect pregnancy; and mutant 3βHSD2 can impair sexual development and induce a severe salt-wasting crisis, resulting in congenital adrenal hyperplasia (*13, 16-19*). Therefore, it is imperative to gain a better understanding of how 3βHSD2 is regulated.

While the actual composition of the adrenal mitochondrial membrane remains unknown, studies have characterized the heart mitochondrial membrane (*16*); we based our studies on the findings. We chose to use dipalmitoylphosphatidylglycerol (DPPG) to mimic the lipid environment (Fig 1B). DPPG is similar in structure to cardiolipin as it has a phosphatidyl moiety, glycerol and acyl chains linked together. As a result, like cardiolipin, DPPG in nature has a large well hydrated head group. Due to this charged nature, DPPG contributes to the maintenance of the electrochemical gradient across membranes, which enables ATP synthesis and ADP-ATP translocation (*17, 18*). Cardiolipin forms hexagonal phases in presence of calcium, but it forms a bilayer under normal condition. We also used dipalmitoylphosphatidylcholine (DPPC). DPPC and DPPG differ only in head group charge and structure. As such, we could compare their behaviors within our model system to isolate the head-group-specific effects due to lipid chain unsaturation. This provides a way to

distinguish between head-group specific protein lipid interactions and to examine whether such interactions can influence the spatial distribution of lipid components within the bilayer.

We found that 3βHSD2 is imported into the IMM by translocases, following synthesis in the cytosol, and once at the IMM, the enzyme is active. The bifunctional activity of 3βHSD2 requires the protein to undergo a conformational change (*19, 20*); the enzyme first exhibits dehydrogenase activity producing NADH, which in turn activates the isomerase activity, but the mechanism underlying the conformational change remains unknown. We hypothesize that 3βHSD2 associates with, but does not integrate into the lipid membrane, and that this results in a conformational change that allows 3βHSD2 to interact with multiple proteins in the intermembrane space.

## MATERIALS AND METHODS

### Reagents

Purified human 3βHSD2 was stored at 4° C in enzyme buffer (20 mM potassium phosphate pH 7, 20% glycerol, 0.1 mM EDTA, 0.01 M $NAD^+$, and 0.4% Igepal). Dansylphosphatidylethanolamine (dansyl-PE) was obtained from Molecular Probes (Invitrogen, Carlsbad, CA). Dipalmitoylphosphatidylcholine (DPPC) and dipalmitoylphosphatidylglycerol (DPPG) were purchased from Avanti Polar Lipids (Birmingham, AL).

### Expression, purification and detergent exchange of human 3βHSD2

3βHSD2 cDNA was introduced into Baculovirus as previously described (*21*). The recombinant Baculovirus was incubated with $2.25 \times 10^9$ Sf9 cells in 1.5 L cells × 6 expressions at a multiplicity of infection of 10. To confirm expression of 3βHSD2, proteins from the Sf9 cells were separated by SDS-polyacrylamide (12%) gel electrophoresis, probed with our anti-3βHSD2 polyclonal antibody (*14*) and detected using the West Pico Western blotting system (Pierce, IL). The expressed enzyme was purified from a 100,000×g pellet of Sf9 cells by our published method (*22, 23*), using Igepal CO 720 (Rhodia, Inc., Cranbury, NJ). SDS-polyacrylamide (12%) gel electrophoresis of the purified enzyme resulted in a single band at 42 kDa that co-migrated with the control 3βHSD2 enzyme. The high- critical micelle concentration (CMC) detergent, Cymal-5 (Anatrace, Inc., Maumee, OH) was exchanged for Igepal using hydroxyapatite chromatography. The 3βHSD2 fraction pool from the DEAE column was applied to the hydroxyapatite column (1 mg protein/ml packed gel), washed with 3.5 column volumes of 0.025 M potassium phosphate, pH 7.5, 20% glycerol, 0.1 mM EDTA, 0.01 M $NAD^+$, 1.8 mM Cymal-5 and then eluted with 0.30 M potassium phosphate, pH 7.5, 20% glycerol, 0.1 mM EDTA, 0.01 M $NAD^+$, 1.8 mM Cymal-5. The peak of 3βHSD2 activity was pooled and found to be free of Igepal CO-720 based on absorbance at 280 nm due to the Igepal CO-720. Protein concentrations were determined by the guanidinum hydrochloride denaturation method (*24*) to avoid errors in extinction coefficients, but the total mitochondrial protein was estimated by the Bradford method using bovine serum albumin as the standard. During enzyme purification, the isomerase activity of 3βHSD2 was measured by the initial absorbance increase at 241 nm- due to androstenedione formation from the intermediate substrate, 5-androstene-3, 17-dione- as a function of time. Blank assays (zero-enzyme, zero-substrate) assured that specific isomerase activity was measured as opposed to non-enzymatic, “spontaneous” isomerization. Changes in absorbance were measured with a Varian (Sugar Land, TX) Cary 300 recording spectrophotometer.

### Biological activity of the purified proteins

Metabolic conversion assays were conducted using mitochondria isolated from mouse Leydig MA-10 cells. To measure the conversion of pregnenolone to progesterone, we incubated 3 million CPM of $^{3}$H-pregnenolone with the isolated mitochondria (20 g) in potassium phosphate buffer and then chased with 30 g of cold progesterone. The reaction, initiated by the addition of 0.01 M $NAD^{+}$, proceeded for 4 h at 37° C in a shaking water bath. Steroids were extracted in ether/acetone (9:1, v/v), and an equal amount of cold pregnenoloneprogesterone (50:50) (Sigma) in $CH_2Cl_2$ was added as a carrier. The steroids were concentrated under nitrogen or by blowing air, and then separated by TLC (Whatman, MA) using chloroform/ethyl acetate (3:1). $^{3}$H-Enhancer was used to enhance the signal intensity, which was measured using a phosphorimager. For an accurate determination of steroid amounts, each spot from the silica plate was scraped and extracted with a solvent mixture of ether: chloroform (3:1); HPLC was performed using an ultrasphere C18 column with a particle size of 5 μm, pore diameter of 80 Å, inner diameter of 4.6 mm and a length of 25 cm; and mass spectrometry was used to characterize tryptic fragments.

### Circular Dichroism (CD)

CD experiments in the far-UV region (185-250 nm) were carried out using a 2.0 mm path-length quartz cuvette at 20° C in a Jasco J-815 spectropolarimeter equipped with a Peltier temperature-controlled cell holder. The instrument was purged with a continuous flow of nitrogen at 10 L/min to reduce the maximum signal to noise ratio. Purified wild-type 3βHSD2 was equilibrated in $Na_2HPO_4$ buffers at pH 7.4, and the CD spectra recorded in the far-UV are presented without mathematical smoothing. The mean residue molar ellipticity [Θ] at 208 and 222 nm was plotted versus lipid concentration. Secondary structural analysis was carried out using the CD-Pro software (*25-28*) to determine the relative proportions of α-helix and β-sheet as a function of lipid concentration, either individually or a mixture of two different lipids. In a separate set of experiments, purified wild-type 3βHSD2 was equilibrated in 10 mM sodium phosphate at pH 7.4 with increasing concentrations of various synthetic lipid vesicles. To evaluate the stability of 3βHSD2, we first measured the wavelength scan dependent unfolding (Θ) at 222 nm at temperatures that increased from 4° C to 80° C. For vesicle effect determination, the vesicles with different compositions were mixed with a fixed concentration of 3βHSD2 at pH 7.4. For each set of measurements, the appropriate buffer blank was subtracted from each spectrum, and Θ at 222 nm was plotted with respect to temperature or vesicle composition.

For thermal denaturation studies, melting curves were obtained by measuring the CD signal at 222 nm as a function of temperature, which ranged from 4° C to 90° C. The temperature was increased 0.5° C per minute. The additive effects of denaturation were determined by the addition of lipids of various compositions with 3βHSD2 after equilibration for 2h.

### Modeling and Sequence Alignment

Amino acid and nucleotide sequences were retrieved from the Swiss Protein Database (*29*). Limited proteolysis with trypsin of the full-length protein was assayed in the presence of DPPC, DPPG, and an equal mixture of DPPC:DPPG. The resulting fragments were analyzed by mass spectrometry and modeled using the Pymol Molecular Graphics system (Version 1.3 Schrodinger, LLC) on the preliminary results (*30, 31*).

### Fingerprinting

To understand the organization of 3βHSD2 domains and to determine differences between the loosely folded domain and the tightly folded domain, we performed proteolysis of the 3βHSD2 protein (5 μg) using a 80 ng of trypsin (sequencing grade, Promega) in the

presence and absence of different lipid vesicles at room temperature or 4° C. The reactions were terminated with an equal volume of SDS-sample buffer containing 2 mM PMSF and then transferred to a boiling water bath after the indicated incubation time. Following electrophoresis, the samples were stained with Coomassie brilliant blue or probed with our 3βHSD2 antibody. Individual bands were excised, destained, reduced with DTT (Roche), alkylated with iodoacetamide (Sigma) and then digested with trypsin (Promega Sequencing Grade Modified) overnight (*32*). The resulting peptides extracted from the gel were analyzed via LC MS/MS on a nanoAcquity HPLC (Waters, MA) coupled with a Q-ToF-Premier mass spectrometer (Micromass, UK / Waters, MA). Peptides were separated using a linear water/acetonitrile gradient (0.1% Formic acid) on a nano Acquity column (3 μm Atlantis dC18, 100 Å pore size, 75 m ID × 10 cm) (Waters, MA), with an in-line Symmetry column (5 μm C18, 180 μm ID × 20 mm) (Waters, MA) as a loading/desalting column. Protein identification from the generated MS/MS spectra was done by searching the NCBI non-redundant database using Mascot MS/MS Ion Search at www.matrixscience.com (Matrix Science, UK) with consideration for carbamidomethylated cysteine and oxidation of methionine.

## Vesicle Preparation

Phospholipids, dissolved in chloroform, were mixed with dansyl-PE (2 mol%) and dried under $N_2$. Samples were then hydrated with 20 mM citrate buffer (pH 7) containing 150 mM KCl to give a 0.33–1 mM final bulk lipid concentration. The hydrated lipids were heated to 50° C to ensure that the mixture was above the lipid phase transition (42° C) temperature and incubated for one hour with intermittent mixing by rapid agitation. The resulting multilamellar vesicles were converted to large unilamellar vesicles by high pressure extrusion at 50° C through a polycarbonate membrane with 100 nm pores as described (*33, 34*).

## Fluorescence Measurements

The binding of 3βHSD2 to phospholipid vesicles was assessed by fluorescence resonance energy transfer using tryptophan residues in the protein as the donor and dansyl-PE in the membrane as the acceptor. Energy transfer was assayed using a photon counting spectrofluorometer (Fluoromax 3, Horiba Scientific, Edison NJ). Excitation was set at the maximum for Trp (280 nm) and the emission of both tryptophan and dansyl-PE were assessed by acquiring an emission spectrum from 400 to 540 nm with a 4 nm band pass. Spectra were confined to this narrow range because optical artifacts contributed by the enzyme buffer precluded obtaining interpretable data at either longer or shorter wavelengths. Samples were equilibrated in the fluorometer sample compartment at 37° C with continuous magnetic stirring. Spectra were then obtained first with vesicles alone (50 μM total lipid concentration), and again after mixing with 3βHSD2 (6 μg/ml final concentration, 5 min equilibration time). Measurements were repeated with excitation set at 340 nm to control for direct effects of the enzyme on the intrinsic dansyl-PE fluorescence. Such effects were generally small. Energy transfer was quantified and corrected for direct effects on intrinsic dansyl-PE fluorescence using the following formula: $relative\quad amount\quad bound = 1 - \frac{a_2}{a_1} \times \frac{b_1}{b_2}$ where $a_1$ = emission intensity of vesicles containing dansyl-PE at 510 nm before addition of enzyme with excitation at 280 nm; $a_2$ = emission intensity at 510 nm after addition of enzyme with excitation at 280 nm; $b_1$ = emission intensity of vesicles at 510 nm before addition of enzyme with excitation at 340 nm; and $b_2$ = emission intensity at 510 nm after addition of enzyme with excitation at 340 nm. Control experiments were also conducted in which enzyme or enzyme buffer was added in the absence of vesicles to assess background fluorescence.

## RESULTS

The conversion of pregnenolone to progesterone and DHEA to androstenedione requires that 3βHSD2 serves as both a dehydrogenase and isomerase. This dual functionality of 3βHSD2 is achieved by a conformational change that shifts the catalysis from dehydrogenase to isomerase. We hypothesized that 3βHSD2 does not need a receptor for interaction at the inner mitochondrial membrane, but rather interacts with nearby lipid vesicles and thereby undergoes the conformational change required for full activity.

### Expression, purification and characterization of the 3βHSD2 protein

Baculovirus-expressed enzyme was purified in the presence of the low-CMC detergent, Igepal CO 720. To provide an enzyme preparation that was suitable for CD analysis, we exchanged Igepal-CO-720 (low CMC , strong UV absorbance at 280 nm) for the high CMC detergent Cymal-5 (no UV absorbance). In fractions probed with the 3βHSD2 antibody, we observed a single band at 42.0 kDa that co-migrated with the crude preparation 3βHSD2 (Fig. 1C). To confirm the biological activity of purified 3βHSD2, we did pregnenolone conversion assays using mitochondria from steroidogenic Mouse Leydig (MA-10) cells. Conversion was initiated with $NAD^+$, and as a control, we included the 3βHSD2 inhibitor, trilostane (5 pmol). As expected, addition of $NAD^+$ resulted in a 20-fold increase in conversion by MA-10 mitochondria and this increase was inhibited by the presence of trilostane (Fig. 1D). The activity was further increased 1.5-fold by the addition of 1.0 g baculovirus-expressed 3βHSD2 protein. The use of heat-inactivated mitochondria blocked conversion, confirming that the additional activity was due to the recombinant 3βHSD2 protein and thus the protein employed in this study was biologically active.

### Lipid Binding of 3βHSD2

To understand the influence of lipid membranes on 3βHSD2, we analyzed 3βHSD2 binding to charged and uncharged unilamellar lipid vesicles by fluorescence resonance energy transfer (FRET). In this technique, a donor chromophore, initially in its electronically excited state, transfers energy to a nearby acceptor chromophore through nonradiative dipole-dipole coupling. The dependency of FRET efficiency on the inverse of the distance, to the sixth power, between acceptor and donor pairs makes this technique useful for monitoring adsorption of molecules to a surface. In these experiments, 3βHSD2 tryptophan (Trp) residues, which are excited at 280 nm, served as the donor while the acceptor was a fluorophore-conjugated phospholipid, dansyl-PE. Figure 2A displays fluorescence emission spectra obtained with enzyme alone (gray), dansyl-PE-doped DPPC vesicles alone (red), and both enzyme and vesicles (blue) after excitation at 280 nm. We observed an increase in intensity, from 450 to 540 nm, due to a modest excitation of dansyl-PE fluorescence. Vesicles that contained 3βHSD2 generated a slightly greater relative intensity than vesicles alone. The optimal excitation wavelength for dansyl-PE is 340 nm and samples excited at this wavelength produced a peak fluorescence emission centered at 510 nm (Fig. 2B). At 340 nm, the presence of 3βHSD2 had no influence on the dansyl-PE fluorescence intensity or wavelength of maximum emission. This modest enhancement of dansyl-PE fluorescence excited at 280 nm by the presence of 3βHSD2 indicates energy transfer from tryptophan in the protein to dansyl-PE in the membrane and implies moderate adsorption of the protein to the membrane surface. The magnitude of the energy transfer efficiency was increased by a factor of five (from a relative transfer efficiency of 0.23 to 1.26) when anionic vesicles (DPPG) were used (Fig. 2C). Repetition of the experiment with vesicles consisting of a 1:1 mixture of DPPC and DPPG gave an intermediate result (Fig. 2D), where the transfer efficiency was 0.50.

### Effect of lipid membrane on 3βHSD2 conformation

Studies have indicated that the environment, including lipid composition, can often influence protein conformation and folding (*36*). Because the previous experiment showed an interaction between 3βHSD2 and lipid membranes, we next tested whether lipid membranes stimulated the protein to adopt a conformation suitable for this interaction. Lipid influence may be particularly pertinent for 3βHSD2 as this protein resides in the inner mitochondrial membrane (*14*). Circular dichroism (CD) spectroscopy can distinguish secondary structural characteristics: The presence of minima near 198 nm indicates random coils, at 208 and 222 nm indicates α-helices, and at 218 nm indicates β-sheets. As the lipid composition changes, flexible domains of the protein bind with the lipid vesicles; thus, an increase in lipid concentration can further alter conformation. In the presence of increasing concentrations of DPPC, from 50 M to 300 M, 3βHSD2 fully retained the α-helical character it exhibited in the absence of lipid (Fig. 3A). In contrast, DPPG altered the wavelength scan CD. The addition of 3.5 M DPPG resulted in a significant change in ellipticity at the $\pi-\pi^*$ transition, 208 nm (Fig 3), suggesting that the protein bound to DPPG because of the polar charged group, leading to protein unfolding. To determine if the degree in reduction in ellipticity was indeed due to the charged vesicles, we measured the helical content after addition of increasing concentrations of a 1:1 mix of DPPC and DPPG, and found similar lipid-dependent unfolding (Fig 3C). Figure 3D shows the analysis of the change in protein conformation. We determined that the wild-type 3βHSD2 protein consisted of approximately 32% α-helix and 25% β sheet, with the remainder as turns. Addition of equal mixture of DPPC and DPPG vesicles up to 5 μM did not alter the α-helical content, but further increases in DPPC:DPPG concentration led to a sharp decrease in the α-helical content, which then reached a plateau at 10% prior to a complete loss of its structure. These results indicate that mixed vesicles bound more strongly to the protein than vesicles consisting solely of a charged phospholipid or zwitterionic lipid membrane. A plot of the helical content as a function of lipid composition shows a cooperative unfolding with increase in lipid composition (Fig 3D). In summary, we did not find any change in α-helical content with DPPC, but a mixture of DPPC and DPPG unfolded 3βHSD2 in the same fashion as DPPG alone. However, the β-sheet content remained unchanged in the presence of DPPC, DPPG or a mixture of both the lipids. This suggests that as the protein unfolded and lost most of its α-helical conformation, it maintained its β-sheet conformation; thus, association with the lipids may affect protein stability.

### Stability of 3βHSD2

The above results revealed destabilization of the protein conformation with increased vesicle concentration. To further evaluate the stability of 3βHSD2, we measured thermal unfolding (Tm) in the presence and absence of lipid membrane. The wavelength scan CD of 3βHSD2 at 20° C resulted in minima at 208 and 222 nm, a typical characteristic of the α-helical conformation. The change in ellipticity at 222 nm was measured in temperatures ranging from 4° to 90° C (Fig 4) and the derivatives ($d\Theta/dT$) plotted as a function of temperature to yield the exact Tm (Fig 4, insets). The protein showed ellipticity changes at or above 40° C and complete denaturation at 60° C. The Tm was 42° C in the absence of lipid (Fig 4A) (shown as inset). 3βHSD2 unfolded in a similar manner in the presence of zwitterionically charged DPPC vesicles (Fig 4B) or an equal mixture of zwitterionic vesicles and anionic vesicles (Fig 4D). The Tm for these conditions was approximately 37° C but a Tm could not be determined in the presence of anionically charged DPPG alone (Fig. 4C). Stability decreased, as indicated by protein unfolding starting at 30° C with complete denaturation at 65° C. The curves are typical for thermal denaturation. Based on our results, we conclude that lipids open the conformation and thus minimally destabilize 3βHSD2 to promote the association of the protein with the vesicles.

## Proteolytic Digestion of 3βHSD2

To understand 3βHSD2 folding in greater detail, we sought to determine whether 3βHSD2 contains domains that are differentially protected from proteolysis by fingerprinting experiments under various conditions. Trypsin is a highly specific enzyme that cleaves protein after lysine and arginine residues under mildly alkaline conditions (at or above pH 7.0). We used trypsin at pH 7.4 to partially digest 3βHSD2 in the absence of lipid, or in the presence of DPPG, DPPC or an equal mixture of DPPC and DPPG. Proteolysis was done at different temperatures for varying lengths of time. The digestion patterns were analyzed by protein staining with Coomassie blue and by Western blotting with 3βHSD2 antiserum along with mass spectrometry (Table 1 and Fig 5). In the absence of any lipids, the protein, especially at lower concentrations of trypsin, 3βHSD2 remained fairly insensitive to digestion and only generated one smaller fragment, designated as Band 1 (Fig 5A). However, in the presence of DPPG, we observed a 30 kDa protein fragment that appeared after incubation for 15 minutes at room temperature (Band 2, Fig 5B). After 30 minutes of incubation, we saw additional discrete tryptic fragments (Bands 3 and 4, Fig 5B), suggesting a tightly packed protein core was formed due to the addition of DPPG. Mass spectrometric analysis of Band 2 from Figure 5B identified amino acids 94-362 of 3βHSD2, suggesting the deletion of the first N-terminal 93 amino acids (Table 1). Thus, association with DPPG resulted in the exposure of the first 93 amino acids of 3βHSD2. Next, we incubated the protein with a mixture of DPPG and DPPC (Fig 5C, Table 2). Proteolysis again produced a 39 kDa fragment (Fig 5C, Band 1) also observed in the absence of lipid (Fig 5A) and in the presence of DPPG (Fig 5B). We also observed Band 2, but this fragment remained stable for less than five minutes and then was further proteolysed to a smaller fragment we termed Band 3. Mass spectrometric analysis of the Band 3 indicated that this fragment consisted of amino acids 94-362 of 3βHSD2, similar to Band 2 seen with DPPG incubation. However, in the presence of DPPC (Fig 5D, Table 3), the stable band consisted of amino acids 274 to 362 (Band 3). As a control we also incubated inner mitochondrial resident cytochrome P450scc with 25 mM lipids and 80 ng of trypsin for 15 and 30 minutes (Fig 5E). P450scc was digested more with increase in time, suggesting that lipid vesicles did not inhibit trypsin activity (Fig 5E). The mass spectrometric results of 3βHSD2 binding with the vesicles are summarized in the form of a diagram showing the protected amino acids from trypsin (Fig 5F). The diagram (Fig 5F) shows that a large C-terminal region was protected from limited proteolytic digestion at pH 7.4 while the N-terminal region, essential for activity, was exposed and hence accessible to proteolysis. When the protein was mixed with charged lipid, the protein's tertiary structure was more collapsed than when it was mixed with the zwitterionic DPPC and charged DPPG. The lipid mixture protected some sites that were not previously protected. Theoretical analysis of 3βHSD2 shows that both of these peptides contained numerous potential cleavage sites for trypsin; thus, the failure of trypsin digestion to cleave these sites at the same pH attests to a substantial change in protein folding and the possibility that these cleavage sites were buried within the lipid membranes.

## Mass spectrometric data fitting with the model

We next examined the influence of lipid membranes on the folding of 3βHSD2 using mass spectrometry. Limited proteolysis with trypsin on the full-length protein was assayed in the presence of DPPC, DPPG, and an equal mixture of DPPC: DPPG. Mass spectrometric data of the protected peptide regions were modeled using the Pymol molecular graphics system (Fig 6 and 7). We performed homology modeling (*30*) based on the short chain oxidoreductase family of enzymes that utilize $NAD^+$ as the preferred cofactor and have an $Asp^{36}$-$Xaa^{37}$ sequence in the first α-β turn of the Rossmann-fold (β-α-β-α-β-α-β-α) (*37, 38*). We matched the fitted mass spectrometric lipid-protein protection results with the known model earlier developed by the Thomas lab (*30*) . The model, regenerated by Pymol Molecular Graphics, shows the presence of 6 β-sheets (Fig 6, red) numbered from 1-6:

1(1-7), 2 (31-36), 3 (57-60), 4 (78-82), 5 (182-184) and 6 (265-263) are located mostly in the N-terminal catalytically active region. The model also shows 12 α-helices, presented as A-L: A(15-26), B(43-56), C(66-75), D(88-93), E(96-115), F(154-174), G(191-200), H(202-207), I (225-238), J (245-253), K (331-335) and L (346-360). The residue for each helix is shown in blue. The unstructured region random coil areas are colored grey. According to the model, most of the β-sheet rich region is buried and forms a hydrophobic cavity where the catalytically important residues, such as D36 and K37, are situated. The cofactor $NAD^+$ and DHEA are shown in orange. These make intimate contacts with D36 and K37, which play an important role in isomerase activity (*39*). When the protein was incubated with trypsin in the absence of lipids, 10 residues of the random coil region were cleaved. The remaining protected region was resistant to protease, even after 60 minutes of incubation (Fig 7A). However, when the protein was incubated with a mixture of the lipids DPPG and DPPC, the protein was digested at the N-terminus. Moreover, protein digested in the presence of either DPPC or DPPG was minimally resistant to proteolytic cleavage (Fig 7B). As indicated in figure 7C, a 93 amino acid segment from the N-terminus was deprotected and cleaved. In this case, β-sheets 1-4 and α-helices A-D and part of the coil regions were cleaved, leaving an exposed cavity in the remaining protected segment. Surprisingly, most of the hydrophobic regions had been cleaved in this event, indicating that this hydrophobic cavity is more exposed in the presence of lipids.

### Membrane influenced activity of 3βHSD2

All the above experiments suggested a strong influence of vesicles in the partial opening of 3βHSD2. To better understand the role of lipid vesicles in enzyme activity, we measured progesterone synthesis by isolated mitochondria in the presence of vesicles (Fig 8). Addition of either charged (DPPG) or zwitterionic (DPPC) lipid did not have much effect, but addition of a mixture of these two vesicles increased the activity almost two-fold (Fig 8, last lane), confirming a role for the vesicles in increasing 3βHSD2 activity. This validates that indeed the mixture of DPPG and DPPC contributes to the activity of 3βHSD2.

## DISCUSSION

Although 3βHSD2 lacks a mitochondrial leader sequence, it appears to be fully functional at the IMM. Based on the observations that the full-length, wild-type 3βHSD2 must undergo unfolding during mitochondrial entry and that the protein becomes active after association with the mitochondrial lipid membrane, we hypothesized that interaction with lipid membrane promotes a partially open conformation of the protein, contributing to 3βHSD2 activity. Multiple findings from this study support this hypothesis, including i) the lipid-dependent unfolding without any change in β-sheet content; ii) the cooperative denaturation with the charged lipid vesicles; iii) the reduction in stability in association with lipid vesicles; iv) the charge-dependent association of the C-terminal domain with lipid vesicles; v) the enhanced adsorption to charged membranes as determined by FRET; vi) the trypsin-mediated cleavage of the catalytically-active N-terminal region only in the presence of lipids; and vii) the lipid-dependent increase in 3βHSD2 metabolic activity. Thus, we conclude that 3βHSD2 activity requires association with membrane vesicles.

In full-length 3βHSD2, the N-terminal mitochondrial leader sequence directs the protein to enter the mitochondrial membrane first, and so we had predicted that the C-terminus would be the region most accessible to proteases. However, we found that the N-terminal 130 amino acids were completely proteolyzed in the presence of either zwitterionic or charged lipid membranes, even though the energy transfer experiments clearly showed better adsorption of the enzyme to charged lipids. The combination of DPPG and DPPC protected most of the protein sequence, except for the first 20 amino acids of the N-terminus. These

first 20 amino acids are hydrophobic and thus the possibility exists that this sequence does not embed into the lipid vesicles, leading to its proteolysis.

The formation of a tightly packed hydrophobic core represents a critical step in the folding pathway of globular proteins. Hydrophilicity analysis shows that the 3βHSD2 sequence is more hydrophilic from amino acid 120 and the amino acid sequence of rest of the protein is weakly hydrophobic and do not form an amphiphilic helix resulting in a favored association with the membrane vesicles. The C-terminal sequence is most likely not cleaved after import through the mitochondrial membrane, but instead remains associated with the lipid membrane. The association may be the result of an electrostatic interaction between the positively charged residues of the C-terminus of the protein and the negatively charged membrane vesicles. At the same time the C-terminal region of 3βHSD2 might need to interact with the vesicle membrane to open its conformation and thus facilitate its activity. In either event, our data suggest that the active form of the 3βHSD2 structure could be preserved in the membrane-associated form (*40*) and as a result, the membrane bound protein retains its compact C-terminus. We hypothesize that this loose N-terminus can quickly associate with the charged membrane, causing the 3βHSD2 protein to pause at the IMM and thus provide more opportunity for 3βHSD2 to remain associated with the membrane, (Fig 7). This might be the critical reason that allows 3βHSD2 to have two different activities at two different steroidogenic steps.

Enzymes catalyzing electron transfer are arranged asymmetrically on the IMM so that protons are translocated across the two mitochondrial membranes. This proton pump establishes an electrochemical gradient where the membrane vesicles facing the IMS side of mitochondria absorb the released protons. 3βHSD2 activity requires $NAD^+$ as a co-activator and disruption of the mitochondrial electrochemical gradient eliminated 3βHSD2-induced activity by mitochondria isolated from mouse Leydig MA-10 cells or pig adrenals. If the interaction of 3βHSD2 with the IMM causes a reduction in the membrane potential ($\Delta\Psi$), our data suggest that this would be at the expense of the flexibility of 3βHSD2 between the protected region of the C-terminus and the charged membrane. As a result, the structure of 3βHSD2 lends itself to partial unfolding, as the short N-terminal and very long C-terminal domains behave differently in the presence of vesicles. Binding with the vesicles correlates well with a lack of extensive flexibility, as indicated by FRET, and strongly suggests a partially open tertiary structure. Thus, partial unfolding induced by the mitochondrial electrochemical gradient and by mitochondrial insertion may result in the transition to a molten globule state. By preserving some secondary structure, the partial open state would provide the best pathway for minimizing the energetic cost of making a compact protein structure able to be inserted into a membrane. Moreover, this transition to a flexible conformation lowers the energy required to open the structure, possibly allowing interactions with other inner mitochondrial translocases or steroidogenic proteins. Thus, 3βHSD2 could function as a dehydrogenase and isomerase for steroidogenesis. In summary, we propose that lipid membranes direct a specific open conformation for 3βHSD2 that could serve as a mandatory step for eliciting its activity on the IMM.

## Supplementary Material

Refer to Web version on PubMed Central for supplementary material.

## Acknowledgments

HSB was supported by a grant from the National Institutes of Health (HD057876), Anderson Cancer Institute and generous support from the MUSM. Funding for equipment in the Mass Spectrometry Facility at the University of Alberta is supported by the Canada Foundation for Innovation and Alberta Science and Research Investment Program. We thank Dr. Gavin P. Vinson, Queen Mary University of London, for providing trilostane.

## Abbreviations

| | |
|---|---|
| **3βHSD2** | 3-beta hydroxysteroid dehydrogenase-2 |
| **Preg** | Pregnenolone |
| **MS** | Mass Spectrometry |
| **FRET** | Fluorescence Resonance Energy Transfer |
| **Mito** | Mitochondria |
| **OMM** | Outer Mitochondrial Membrane |
| **IMM** | Inner Mitochondrial Membrane |
| **DPPC** | Dipalmitoylphosphatidylcholine |
| **DPPG** | Dipalmitoylphosphatidylglycerol |
| **VDAC** | Voltage Dependent Anion Channel |
| **DHEA** | Dehydroepiandrosterone |
| **CD** | Circular Dichroism |
| **IMS** | Intermembrane Space |
| **P450scc** | Cytochrome P450 side chain cleavage enzyme |

## References


1. Neupert W, Herrmann JM. Translocation of proteins into mitochondria. Annu Rev Biochem. 2007; 76:723–729. [PubMed: 17263664]
2. Van der Laan M, Meinecke M, Dudek J, Hutu DP, Lind M, Perschil I, Guiard B, Wagner R, Pfanner N, Rehling P. Motor-free mitochondrial preseqence translocase drives membrane integration of preproteins. Nat Cell Biol. 2007; 9:1152–1159. [PubMed: 17828250]
3. Glick BS, Brandt A, Cunningham K, Muller S, Hallberg RL, Schatz G. Cytochrome c1 and b2 are sorted to the intermembrane space of yeast mitochondria by a stop-transfer mechanism. Cell. 1992; 69:347–357.
4. Tamm LK, Hong H, Linag B. Folding and assembly of β-barrel membrane proteins. Biochem Biophys Acta. 2004; 1666:250–263. [PubMed: 15519319]
5. Walther DM, Papic D, Bos MP, Tommassen J, Rapaport D. Signals in bacterial β-barrel proteins are functional in eukaryotic cells for targeting to and assembly in mitochondria. Proc Natl Acad Sci USA. 2009; 106:2531–2536. [PubMed: 19181862]
6. Kemper C, Habib SJ, Engl G, Heckmeyer P, Dimmer KS, Rapaport D. Integration of tail-anchored proteins into the mitochondrial outer mebrane does not require any known protein import components. J Cell Sci. 2008; 121:1990–1998. [PubMed: 18495843]
7. Chacinska A, Koehler CM, Milenkovic D, Lithgow T, Pfanner N. Importing mitochonrial proteins: machineries and mechansims. Cell. 2009; 138:628–644. [PubMed: 19703392]
8. Claypool SM, Oktay Y, Boontheung P, A LJ, Koehler CM. Cardiolipin defines the interactome of the major ADP/ATP carrier protein of the mitochondrial inner membrane. J Cell Biol. 2008; 182:937–950. [PubMed: 18779372]
9. Kutik S, Rissler M, Guan XL, Guiard B, Shui G, Gebert N, Heacock PN, Rehling P, Dowhan W, Wenk MR, Pfanner N, Wiedemann N. The translocator maintenance protein Tam41 is required for mitochondrial cardiolipin biosynthesis. J Cell Biol. 2008; 183:1213–1221. [PubMed: 19114592]
10. Ardail D, Lerme F, Louisot P. Involvement of contact sites in phosphatidylserine import into liver mitochondria. J Biol Chem. 1991; 266:7978–7981. [PubMed: 2022626]
11. Ardail D, Privat JP, Egret-Charlier M, Levrat C, Lerme F, Louisot P. Mitochondrial contact sites. Lipid composition and dynamics. J Biol Chem. 1990; 265:18797–18802. [PubMed: 2172233]

12. Emoto K, Kuge O, Nishijima M, Umeda M. Isolation of a chinese hamster ovary cell mutant defective in intramitochondrial transport of phosphatidylserine. Proc Natl Acad Sci USA. 1999; 96:12400–12405. [PubMed: 10535934]
13. Simard J, Ricketts M-L, Gingras S, Soucy P, Feltus FA, Melner MH. Molecular biology of the 3β-hydroxysteroid dehydrogenase/Δ5-δ4 isomerase gene family. Endocr Rev. 2005; 26:525–582. [PubMed: 15632317]
14. Pawlak KJ, Prasad M, Thomas TL, Whittal RM, Bose HS. Inner mitochondrial translocase Tim50 interacts with 3beta-hydroxysteroid dehydrogenase type-2 to regulate adrenal and gonadal steroidogenesis. J Biol Chem. 2011; 286:39130–39140. [PubMed: 21930695]
15. Rainey WE, Carr BR, Sasano H, Suzuki T, Mason JI. Dissecting human adrenal androgen production. Trends Endocrinol Metab. 2002; 13:234–239. [PubMed: 12128283]
16. Daum G. Lipids of mitochondria. Biochim Biophys Acta. 1985; 822:1–42. [PubMed: 2408671]
17. Lenaz G, Genova ML. Kinetics of integrated electron transfer in the mitochondrial respiratory chain: random collisions vs. solid state electron channeling. Am J Physiol Cell Physiol. 2007; 292:1221–1239.
18. Christinsen K, Bose HS, Harris FM, Miller WL, Bell JD. Binding of StAR to synthetic membranes suggests an active molten globule. J Biol Chem. 2001; 276:17044–17051. [PubMed: 11279152]
19. Thomas JL, Frieden C, Nash WE, Strickler RC. An NADH-induced conformational change that mediates the sequential 3β-hydroxysteroid dehydrogenase/isomerase activities is supported by affinity labeling and the time-dependent activation of isomerase. J Biol Chem. 1995; 270:21003–21008. [PubMed: 7673125]
20. Thomas JL, Boswell EL, Scaccia LA, Pletnev V, Umland TC. Identification of key amino acids responsible for the substantiality higher affinities type 1 3β-hydroxysteroid dehydrogenase/isomerase (3βHSD1) for substrates, coenzymes and inhibitors relative to 3βHSD2. J Biol Chem. 2005; 280:21321–21328. [PubMed: 15797861]
21. Thomas JL, Evans BW, Blanco G, Mercer RW, Mason JI, Adler S, Nash WE, Isenberg KE, Strickler RC. Site-directed mutagenesis identifies amino acid residues associated with the dehydrogenase and isomerase activities of human type I (placental) 3β-hydroxysteroid dehydrogenase/isomerase. J Steroid Biochem. 1998; 66:327–334.
22. Thomas JL, Myers RP, Strickler RC. Human placental 3 •-hydroxy-5-ene-steroid dehydrogenase and steroid 5-ene • 4-ene-isomerase: purification from mitochondria and kinetic profiles, biophysical characterization of the purified mitochondrial and microsomal enzymes. Steroid Biochem. 1989; 33:209–217.
23. Thomas JL, Mason JI, Brandt S, Spencer BR, Norris W. Structure/function relationships responsible for the kinetic differences between human type 1 and Type 2 3-Hydroxysteroid Dehydrogenase and for the catalysis of the Type 1 Activity. J Biol Chem. 2002; 277:42795–42801. [PubMed: 12205101]
24. Gill SC, von Hippel PH. Calculation of protein extinction coefficients from amino acid sequence data. Anal Biochem. 1989; 182:319–326. [PubMed: 2610349]
25. Sreerama N, Venyaminov SY, Woody RW. Estimation of secondary structure from circular dichroism spectra: inclusion of denatured proteins with native proteins in the analysis. Anal Biochem. 2000; 287:243–251. [PubMed: 11112270]
26. Sreerama N, Woody RW. A self-consistent method for the analysis of protein secondary structure from circular dichroism. Anal Biochem. 1993; 209:32–44. [PubMed: 8465960]
27. Sreerama N, Woody RW. Estimation of protein secondary structure from CD spectra: Comparison of CONTIN, SELCON and CDSSTR methods with an expanded reference set. Anal Biochem. 2000; 282:252–260. [PubMed: 11112271]
28. Sreerama N, Woody RW. Computation and analysis of protein circular dichroism spectra. Methods Enzymol. 2004; 383:318. Ch.13. [PubMed: 15063656]
29. Bairoch A, Apweiler R. The SWISS-PROT protein sequence database and its supplement TrEMBL in 2000. Nucleic Acid Res. 2000; 28:45–48. [PubMed: 10592178]
30. Thomas JL, Duax WL, Addlagatta A, Brandt S, Fuller RR, Norris W. Structure/function relationships responsible for coenzyme specificity and the isomerase activity of human type 1 3β-hydroxysteroid dehydrogenase/isomerase. J Biol Chem. 2003:35483–35490. [PubMed: 12832414]

31. Pletnev VZ, Thomas JL, Rhaney FL, Holt LS, Scaccia LA, Umland TC, Duax WL. Rational proteomics V: Structure-based mutagenesis has revealed key residues responsible for substrate recognition and catalysis by the dehydrogenase and isomerase activities in human 3β-hydroxysteroid dehydrogenase/isomerase type 1. J Steroid Biochem Mol Biol. 2006; 101:50–60. [PubMed: 16889958]
32. Rosenfeld J, Capdeville J, Guillemot JC, Ferrara P. In-gel digestion of proteins for internal sequence analysis after one- or two-dimensional electrophoresis. Anal Biochem. 1992; 203:173–179. [PubMed: 1524213]
33. Bell JD, Burnside M, Owen JA, Royall ML, Baker ML. Relationships between bilayer structure and phospholipase $A_2$ activity: interactions among temperature, diacylglycerol, lysolecithin, palmitic acid and dipalmitoylphosphatidycholine. Biochemistry. 1996; 35:4945–4955. [PubMed: 8664287]
34. Dowhan W, Bogdanov M. Lipid-dependent membrane protein topogenesis. Annu Rev Biochem. 2009; 78:515–540. [PubMed: 19489728]
35. Miller WL, Auchus RJ. The molecular biology, biochemistry, and physiology of human steroidogenesis and its disorders. Endocr Rev. 2011; 32:81–151. [PubMed: 21051590]
36. Gohil VM, Greenberg ML. Mitochondrial membrane biogenesis: phospholipids and proteins go hand in hand. J Cell Biol. 2009; 184:469–472. [PubMed: 19237595]
37. Huang YW, Pineau I, Chang HJ, Azzi A, Bellemare V, Laberge S, Lin SX. Critical residues for the specificity of cofactors and substrates in human estrogenic 17beta-hydroxysteroid dehydrogenase 1: variants designed from the three-dimensional structure of the enzyme. Mol Endocrinol. 2001; 15:2010–2020. [PubMed: 11682630]
38. Duax WL, Pletnev V, Addlagatta A, Bruenn JJ, Weeks CW. Rational proteomics I. Fingerprint identification and cofactor specificity in the short-chain oxidoreductase (SCOR) enzyme family. Proteins Struct Funct Genet. 2003; 53:931–943. [PubMed: 14635134]
39. Thomas JL, Mack VL, Sun J, Terrell JR, Bucholtz KM. The functions of key residues in the inhibitor, substrate and cofactor sites of human 3β-hydroxysteroid dehydrogenase type 1 are validated by mutagenesis. J Steroid Biochem Molec Biol. 2010; 120:192–199. [PubMed: 20420909]
40. van der Goot FG, González-Mañas JM, Lakey JH, Pattus F. A ‘molten-globule’ membrane-insertion intermediate of the pore-forming domain of colicin A. Nature. 1991; 354:408–410. [PubMed: 1956406]

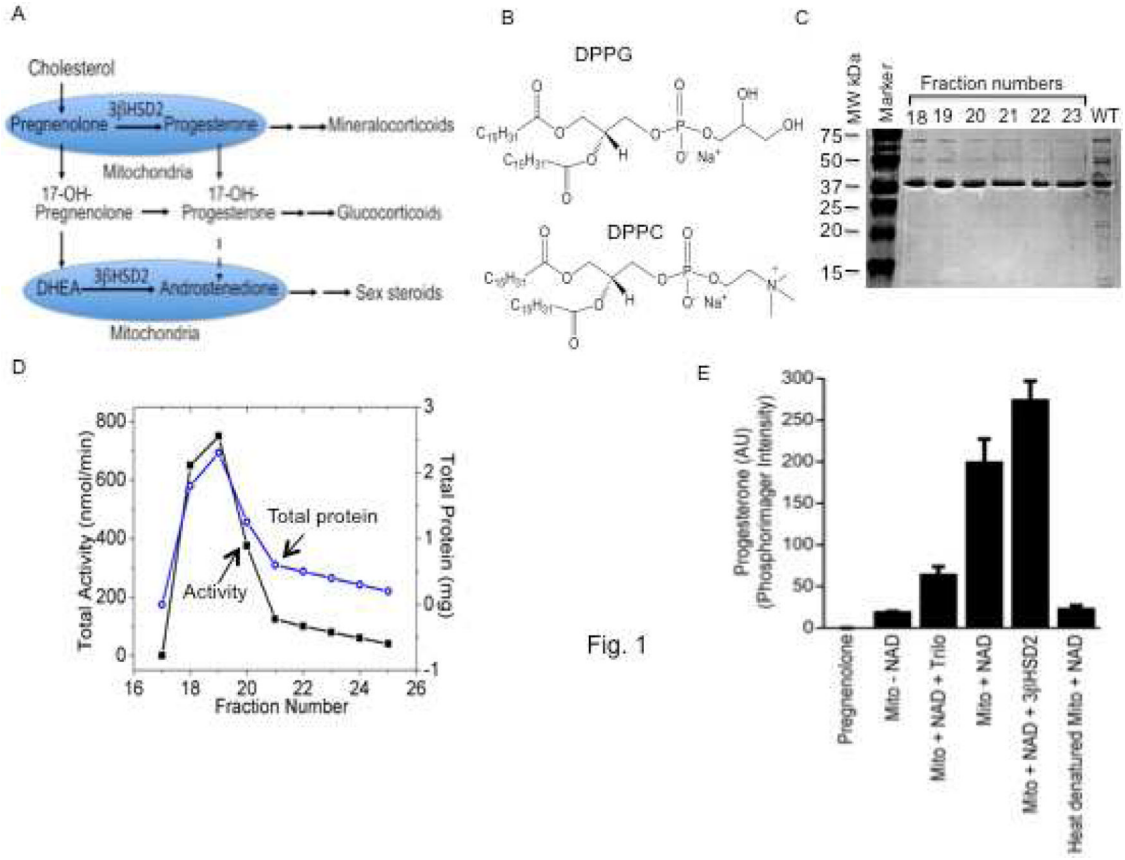


Fig. 1

**Figure 1.**

Expression and purification of the active form of 3βHSD2. Panel (A), schematic presentation of steroidogenesis showing specific regions of 3βHSD2 activity in the mitochondria. Panel (B), the chemical structures of the zwitterionic lipid, DPPC, and the charged lipid, DPPG. Panel (C), expression profile of Baculovirus-expressed 3βHSD2 purified from Sf9 cells through a gel filtration column and stained with Coomassie blue. The crude expression is designated as WT. The lane numbers show the purification pattern. Panel (D), the activity of 3βHSD2 was determined by a direct metabolic conversion assay using $^{3}$H-pregnenolone and mitochondria isolated from the MA-10 cells. The addition of 0.01 M $NAD^{+}$ initiated the reaction and the 3βHSD2 inhibitor, Trilosane (Trilo), abrogated the reaction. External addition of 3βHSD2 increased activity above what was seen at the endogenous level.

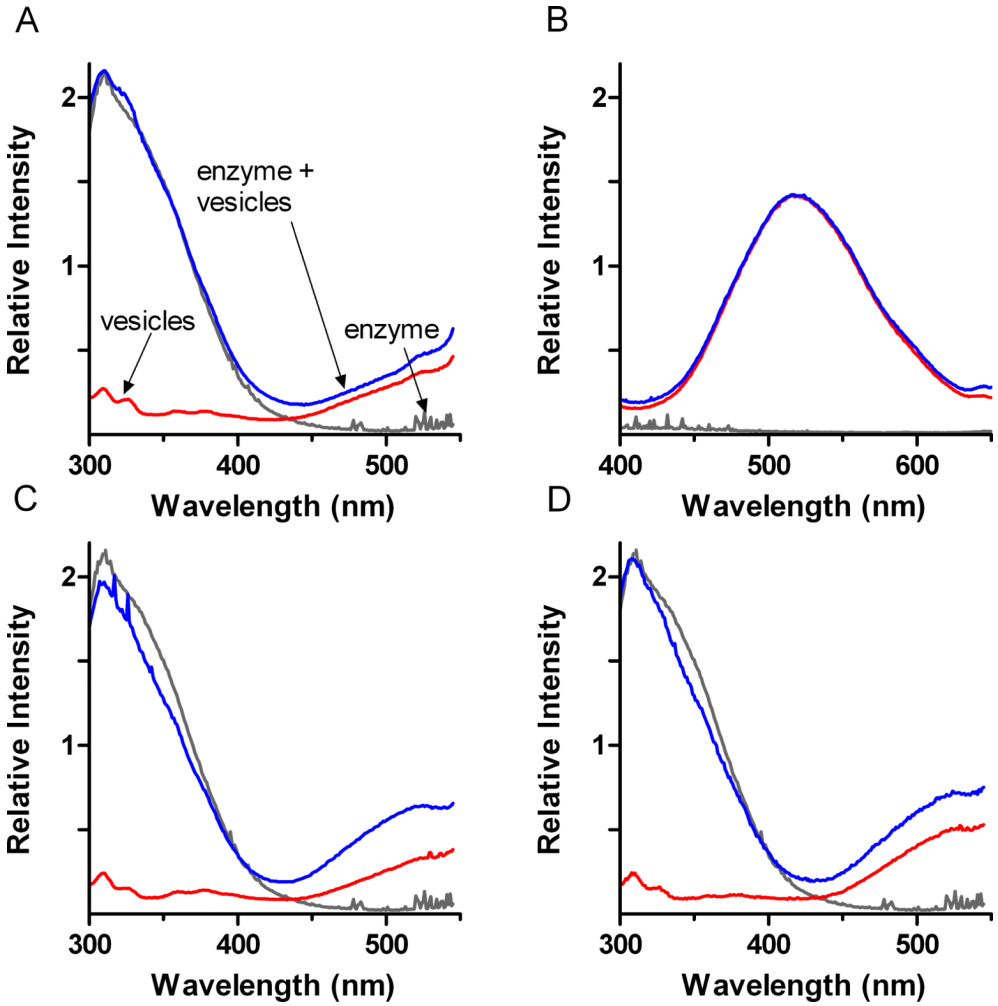


**Figure 2.**

Adsorption of 3βHSD2 to lipid membranes as assessed by FRET. Panel (A), the fluorescence emission spectra, after excitation at 280 nm, was acquired independently for DPPC vesicles doped with dansyl-PE (red curve) or 3βHSD2 (gray curve). The spectrum obtained from a mixture of the two is illustrated by the blue curve. The relative efficiency of energy transfer was calculated with eq. 1 and equal to 0.23 for this experiment. Panel (B), the spectra of (A) were reacquired with excitation at 340 nm. The experiment from (A) was repeated with vesicles composed of DPPG (C) or a 1:1 mixture of DPPG and DPPC (D). Data presented in all panels are the mean ± SEM from three independent experiments performed in triplicate.

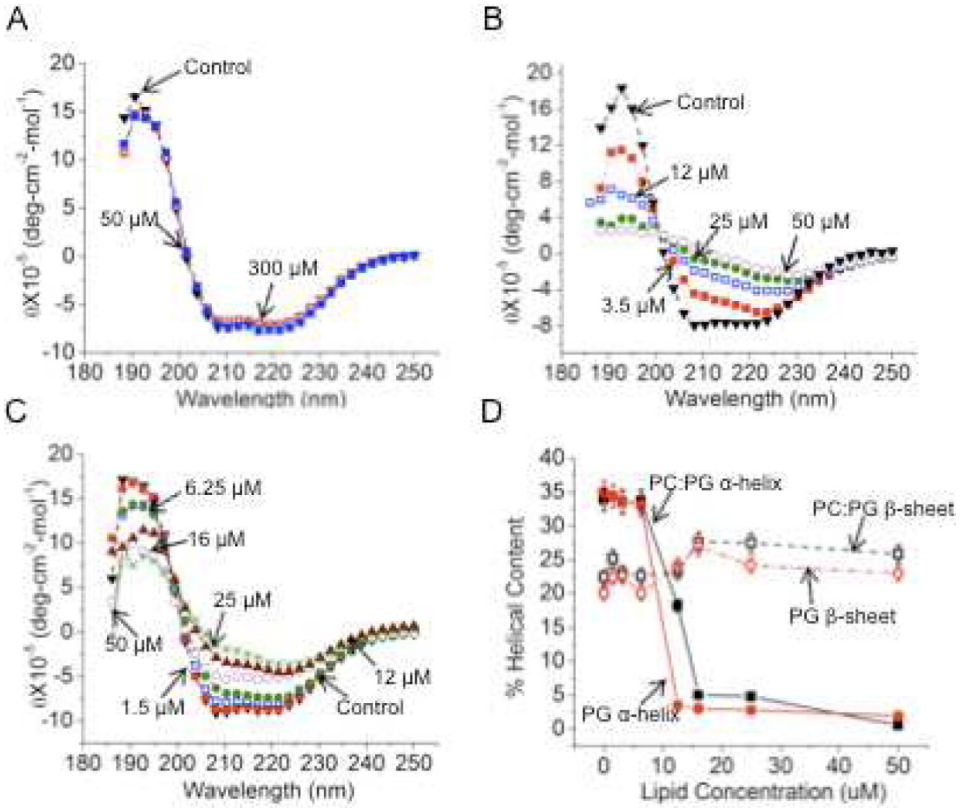


**Figure 3.**

Wavelength scan CD spectra of 3βHSD2 in the presence of different unilameller lipid membranes. Panel (A), wavelength scan CD of 3βHSD2 in the presence of no lipids (Solid inverse triangle in black), 50 μM (Solid square in blue) and 300 μM (Hollow square in red) DPPC from 185 to 250 nm. In all conditions, we observed minima at 208 and 222 nm. There were subtle differences in ellipticity change at 208 nm with 300 μM of DPPC. Panel (B), wavelength scan CD spectra of 3βHSD2 with different concentrations of DPPG from 3.5 (Solid square in red), 12.5 (Hollow square in blue), 25.0, (Solid round circle in green), 50 (Hollow round circle in magenta) μM. The ellipticity minima was reduced with increasing DPPG; first at 208 nm and then at 222 nm, suggesting unfolding of the 3βHSD2 protein, starting at 6.25 mM DPPG. Panel (C), Wavelength scan of 3βHSD2 with an equal mixture of DPPC:DPPG, in the absence of lipid (Solid inverse triangle in black), 1.5 μM (Solid square in red), 6.25 μM (Hollow square in blue), 12 (Solid round circle in green), 16 μM (Hollow round circle in purple), 25.0 μM (Solid triangle in brown), 50 μM (Hollow round circle in green). Unlike individual lipids, lipid mixture caused similar unfolding of 3βHSD2. Panel (D) is a representation of Panels B and C showing analysis of the change in α− helical and β− sheet conformation. The lipid concentrations in Panel B were 3.5 μM, 12.5 μM, 25 μM and 50 μM and in Panel C were 1.5 μM, 6.25 μM, 15 μM and 25 μM. The result shows addition of DPPG or a mixture of DPPG and DPPC reduced the α-helical content to a similar level, but DPPC had no effect. There was no significant change in β-sheet conformation in the above conditions.

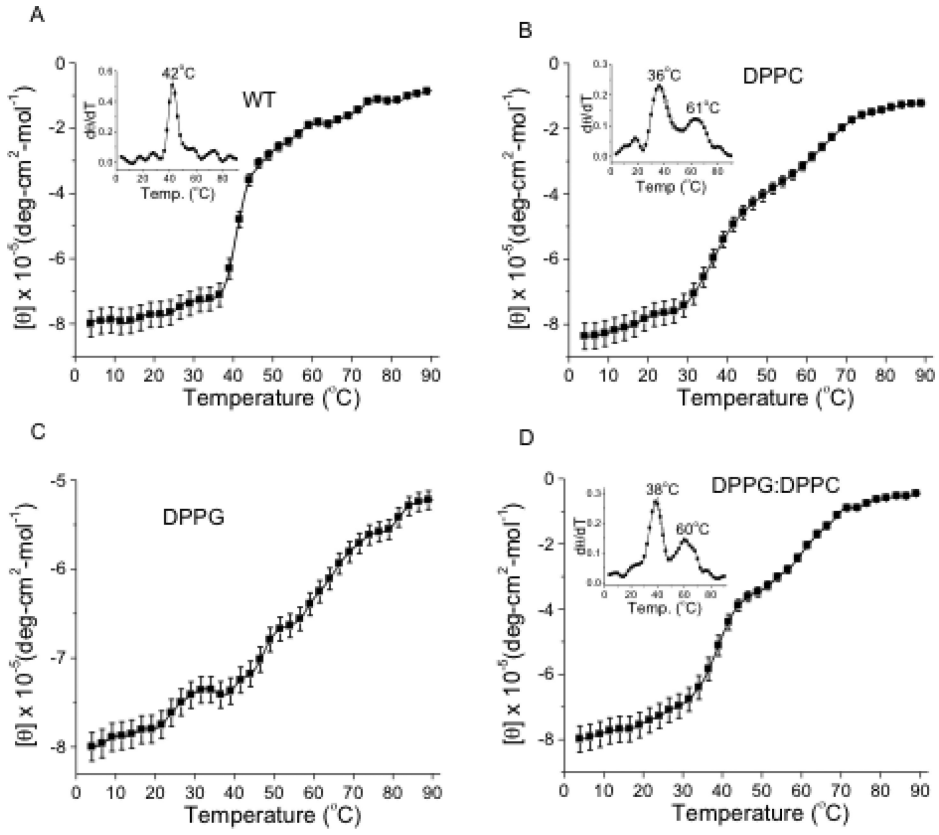


**Figure 4.**

Thermal unfolding (Tm) of 3βHSD2 in the presence and absence of lipid vesicles (25 μM). Thermal denaturation was measured in a CD spectrophotometer by monitoring the ellipticity at 222 nm. We precisely identified the Tm using the derivative dΘ/dT. Panel (A), measurement of 3βHSD2 stability based on Tm. The inset shows the derivative dΘ/dT with a peak at 42° C. Panel (B) thermal unfolding of 3βHSD2 in the presence of DPPC, the inset shows the Tm was 36° C. Panel (C), no thermal unfolding was observed in the presence of DPPG. Panel (D), thermal unfolding of 3βHSD2 in the presence of a mixture of DPPG and DPPC, where the Tm was 38° C. Data presented in all panels are the mean ± SEM from three independent experiments performed in triplicate.

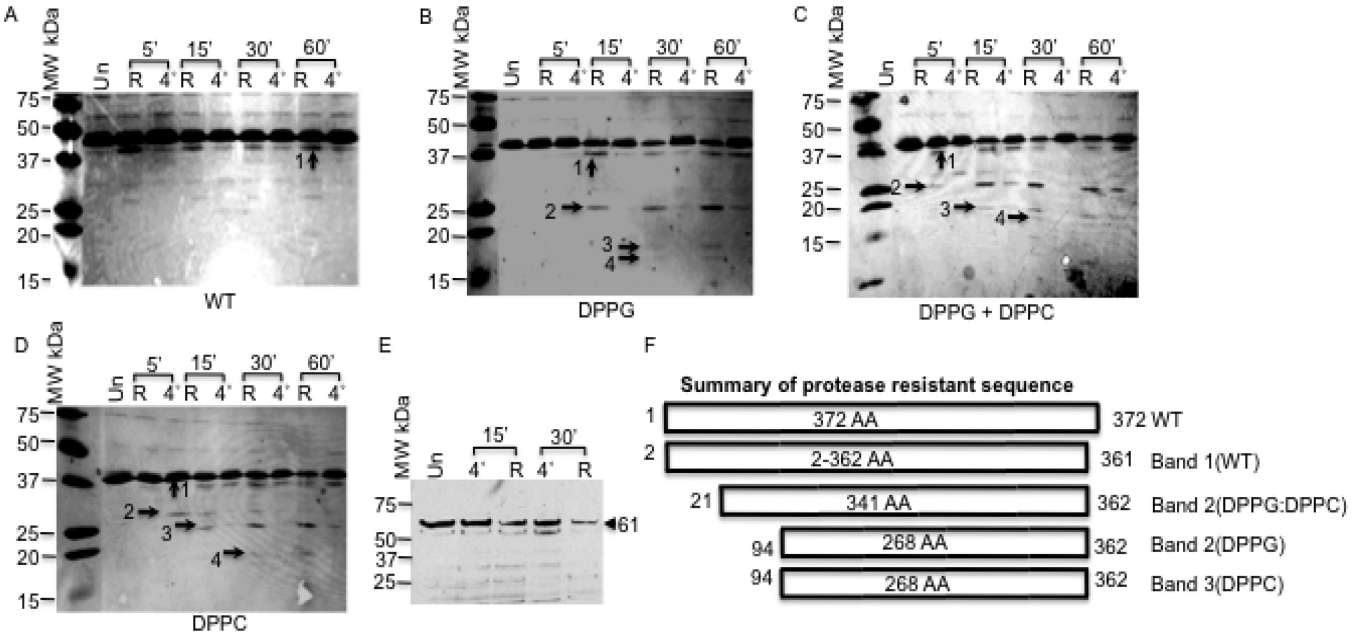


**Figure 5.**

Proteolysis of 3βHSD2 in presence and absence of lipids (25 μM). 3βHSD2 (5 μg) was incubated with 80 ng of trypsin at 4° C (4) or room temperature (R) from 5 to 60 minutes. The first lane shows the undigested (Un) protein applied for each digestion. The samples were electrophoresed on a 17% acrylamide gel and stained with Coomassie blue. Panel (A) is without addition of any lipids, Panel (B) with DPPG, Panel (C) Mixture of DPPC with DPPG and Panel (D) with DPPC. The proteolysis was carried out under identical conditions as indicated in the figure. The protected bands, indicated with arrowhead, were excised for mass spectrometric analysis. Panel (E), proteolytic digestion of cytochrome P450scc after incubation with equal mixture of DPPG and DPPC (25 μM) with trypsin for 15 and 30 min. Panel (F), cartoon describes summary of the mass spectrometric analysis of the trypsin protected bands.

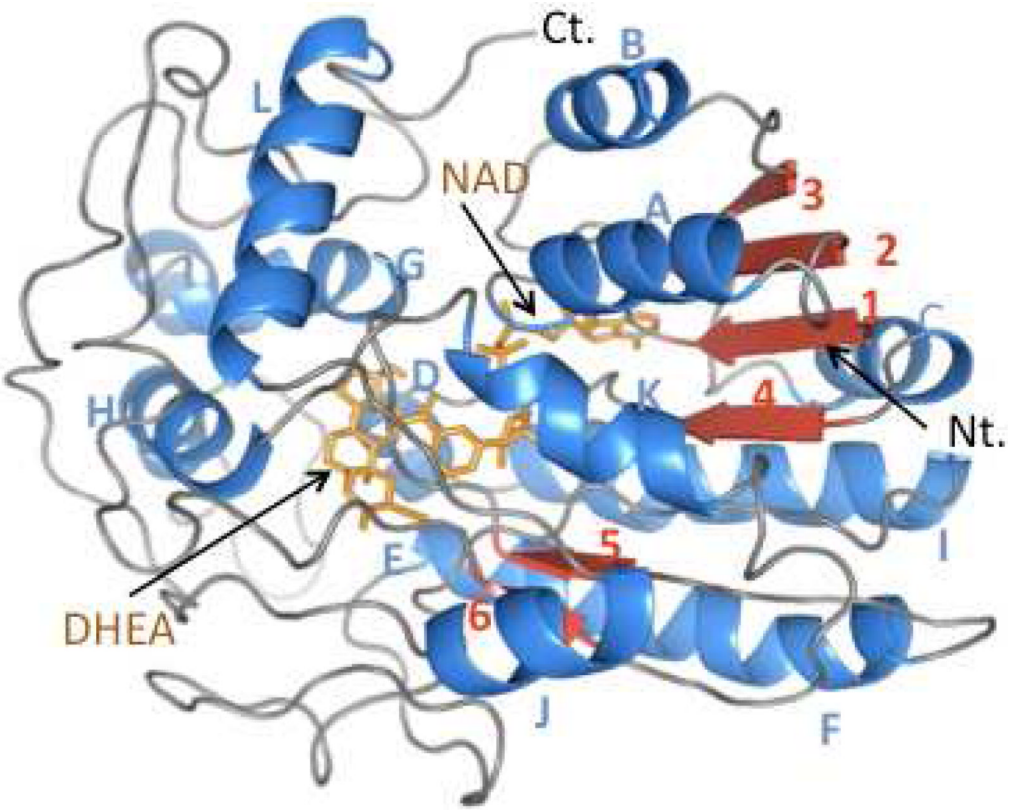


**Figure 6.**

Mass Spectrometric data analysis with the 3βHSD2 structure. Ribbon diagram of human 3βHSD2 isomerase. The diagram was based on homology modeling using UDP-galactose-4-epimerase as a template. The figure was regenerated using the Pymol molecular graphics system. The protein consists of 6 β-sheets: 1 (residues 1-7), 2 (31-36), 3 (57-60), 4 (78-82), 5 (182-184) and 6 (265-267), which are colored in red. There are also 12 α-helices: A (residue 15-26), B (43-56), C (66-75), D (88-93), E (96-115), F (154-174), G (191-200), H (202-207), I (225-238), J (245-253), K (331-335) and L (346-360), which are shown in blue. Peptide segments with non-regular random coil are shown in grey. The active site bound with $NAD^+$ and DHEA are shown in orange.

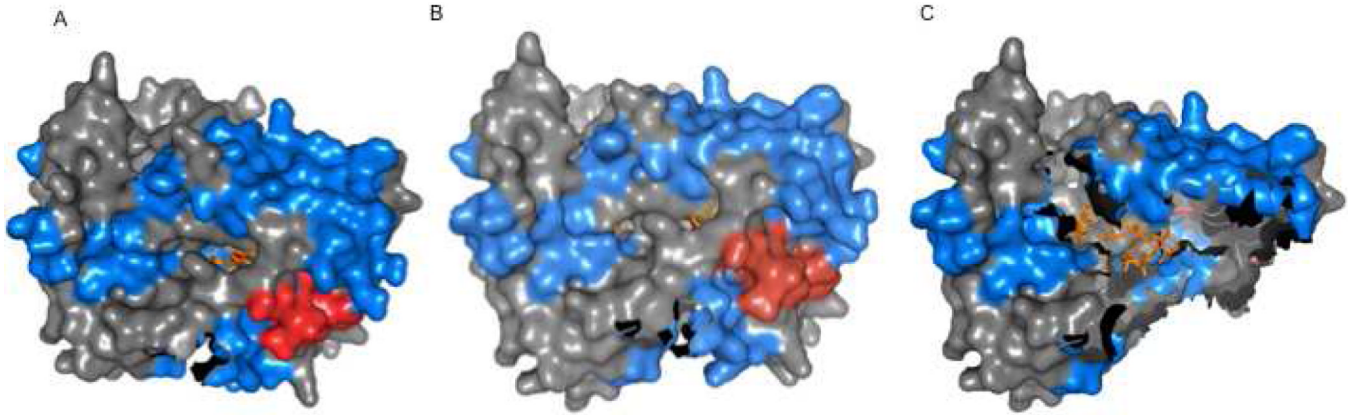


**Figure 7.**

Illustration of trypsin-digested segments (cavity) and the protected segments in the space filling model. Panel (A), Band 1 of 3βHSD2 in the absence of lipids. The cavity shows the cleavage site of C-terminus 10 residues. Panel (B), Band 2 of 3βHSD2 in the presence of DPPG and DPPC. The cavity illustrates the cleavage of 20 amino acids from the N-terminus. The active site is partially open. Panel (C), Band 3 of 3βHSD2 in the presence of DPPC or DPPG. The first N-terminal 93 amino acids were deleted, generating a cavity. The active site remained open and almost all of the β-sheet region was cleaved off.

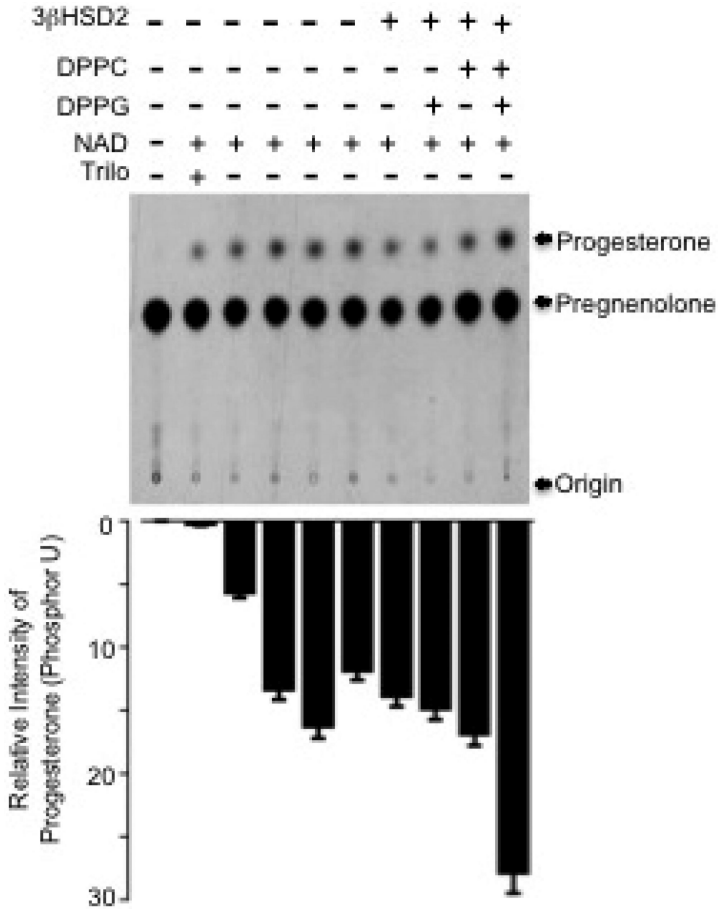


**Figure 8.**

Metabolic conversion in presence lipid vesicles. Metabolic conversion of accumulated pregnenolone to progesterone by mitochondria isolated from MA-10 cells in the presence of 25 μM of DPPC, DPPG or a mixture of DPPG. Metabolic conversion occurred after the addition of $NAD^+$ while the 3βHSD2 inhibitor, trilostane, abrogated catalysis. External addition of 25 μM DPPG and DPPC did not increase activity above the basal level, but addition of a mixture of DPPG and DPPC increased activity two-fold more than what was seen with the mitochondria incubated with $NAD^+$ only.